

Steering and isotope effects in the dissociative adsorption of $\text{H}_2/\text{Pd}(100)$

Axel Gross and Matthias Scheffler

Fritz-Haber-Institut, Faradayweg 4-6, D-14195 Berlin-Dahlem, Germany

Abstract. The interaction of hydrogen with many transition metal surfaces is characterized by a coexistence of activated with non-activated paths to adsorption with a broad distribution of barrier heights. By performing six-dimensional quantum dynamical and classical molecular dynamics calculations using the same potential energy surface derived from *ab initio* calculations for the system $\text{H}_2/\text{Pd}(100)$ we show that these features of the potential energy surface lead to strong steering effects in the dissociative adsorption dynamics. The adsorption dynamics shows only a small isotope effect which is purely due to the quantum nature of hydrogen.

1 Introduction

It is a long-term goal in surface science to understand catalytic reactions occurring at surfaces. Obviously, the single steps of these often rather complicated processes are more effectively studied at simple systems. The dissociative adsorption of molecules on surfaces is one of the fundamental reaction steps occurring in catalysis. This establishes its technological relevance and importance. In particular, the dissociative adsorption and associative desorption of hydrogen on metal surfaces has served as a benchmark system, both experimentally and theoretically (see, e.g., Refs. [1, 2, 3, 4] and references therein). Since the mass mismatch between hydrogen and a metal substrate is rather large, the crucial process in the dissociative adsorption for these particular systems is the conversion of translational and internal energy of the hydrogen molecule into translational and vibrational energy of the adsorbed hydrogen atoms. If in addition no surface rearrangement occurs upon adsorption, the substrate degrees of freedom can be neglected and the dissociation dynamics can be described in terms of potential energy surfaces (PES) which take only the molecular degrees of freedom into account.

The PES for the dissociative adsorption of a diatomic molecule neglecting the substrate degrees of freedom is still six-dimensional. These PESs now become available by elaborate density-functional calculations [5, 6, 7, 8, 9]. However, in order to understand the reaction dynamics one has to perform dynamical calculations on these potentials. Because of its light mass hydrogen has to be described quantum mechanically. Only recently it has become possible to perform dynamical calculations of the dissociative adsorption and associative desorption where *all* degrees of freedom of the hydrogen molecule are treated quantum mechanically [10]. These calculations have established the importance of high-dimensional effects in the reaction dynamics.

For example, molecular beam experiments of the dissociative adsorption of H_2 on various transition metal surfaces like Pd(100) [11], Pd(111) and Pd(110) [12], W(111) [13], W(100) [13, 14, 15], W(100)-c(2×2)Cu [16] and Pt(100) [17] revealed that the sticking probability in these systems initially decreases with increasing kinetic energy of the beam. High-dimensional quantum dynamical calculations have shown that steering effects can cause such an initial decrease in the sticking probability [10, 18]; it is not necessarily due to a precursor mechanism, as was widely believed.

So far we have studied, besides the steering effect [10], the influence of the molecular rotation and orientation [10, 19] and vibration [20] on the sticking probability of $\text{H}_2/\text{Pd}(100)$. In this paper we present a comparison of quantum and classical dynamics for the dissociation of hydrogen on Pd(100) and investigate isotope effects. In the next section the theoretical background will be introduced before the results of the dynamical calculations will be discussed.

2 Theoretical background

The potential energy surface of $\text{H}_2/\text{Pd}(100)$ has been determined using density-functional theory together with the generalized gradient approximation (GGA) [21] and the full-potential linear augmented plane wave method [22, 23]. *Ab initio* total energies have been evaluated for more than 250 configurations [7] and have been parametrized in a suitable form for the dynamical calculations [10].

Figure 1 shows a cut through the PES of $\text{H}_2/\text{Pd}(100)$, where the most favourable path towards dissociative adsorption is marked by the dashed line. For this path there is no energy barrier hindering dissociation, i.e., the adsorption is non-activated. However, the majority of pathways towards dissociative adsorption has in fact energy barriers with a rather broad distribution of heights and positions, as the detailed total-energy calculations showed [7], i.e. the PES is strongly anisotropic and corrugated. This has important consequences, as will be shown below.

The quantum dynamics is determined in a coupled-channel scheme within the concept of the *local reflection matrix* (LORE) [24]. This numerically very stable method is closely related to the logarithmic derivative of the solution matrix and thus avoids exponentially increasing outgoing waves which could cause numerical instabilities. The reported calculations, which take all degrees of freedom of the hydrogen molecule into account, are still only possible if all symmetries of the scattering problem are utilized.

The classical trajectory calculations are performed on *exactly the same* PES as the quantum dynamical calculations. The equations of motions are numerically integrated with the Bulirsch-Stoer method with a variable time-step [25]. The energy conservation is typically fulfilled to 0.1 meV. The sticking probability is determined by averaging over a sufficient number of trajectories. The exact number of trajectories depends on the specific initial conditions and ranges between 1,815 and 18,330.

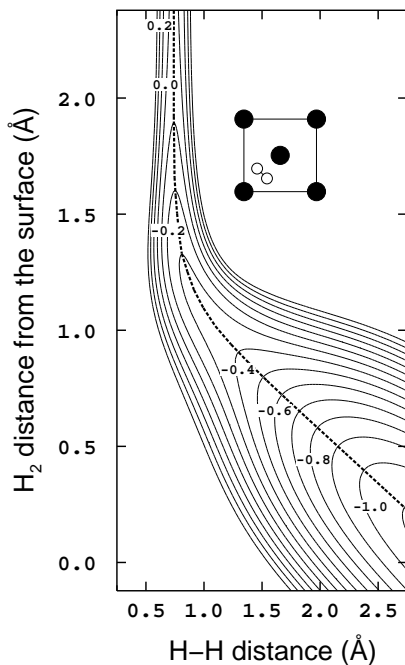


Fig. 1. Contour plot of the PES along a two-dimensional cut through the six-dimensional coordinate space of $\text{H}_2/\text{Pd}(100)$. The inset shows the orientation of the molecular axis and the lateral H_2 center-of-mass coordinates. The coordinates in the figure are the H_2 center-of-mass distance from the surface Z and the H-H interatomic distance d . The dashed line is the optimum reaction path. Energies are in eV per H_2 molecule. The contour spacing is 0.1 eV.

As far as the CPU time requirement is concerned, it is a wide-spread believe that classical methods are much less time-consuming than quantum ones. This is certainly true if one compares the computational cost of one trajectory to a quantum calculations. However, if one is interested in averaged quantities like sticking probabilities, then in classical molecular dynamics calculations one has to average over many trajectories corresponding to different initial conditions. Quantum mechanics does this averaging automatically. A plane wave describing the incident beam hits the surface everywhere, and a $j = 0$ rotational state contains all molecular orientations. Thus for the results presented here the quantum method is even more time-efficient than the classical calculations, in particular if one considers the fact, that in a coupled-channel method the sticking and scattering probabilities of all open channels are determined simultaneously.

3 Results and Discussion

Figure 2 presents six-dimensional quantum dynamical calculations of the sticking probability as a function of the kinetic energy of a H_2 beam under normal incidence on a $\text{Pd}(100)$ surface and five-dimensional calculations for D_2 . In addition, the results of a H_2 molecular beam experiment are shown [11]. Quantum mechanically determined sticking probabilities for hydrogen at surfaces with an attractive well exhibit an oscillatory structure as a function of the incident energy [10, 18, 26, 27], reflecting the opening of new scattering channels and

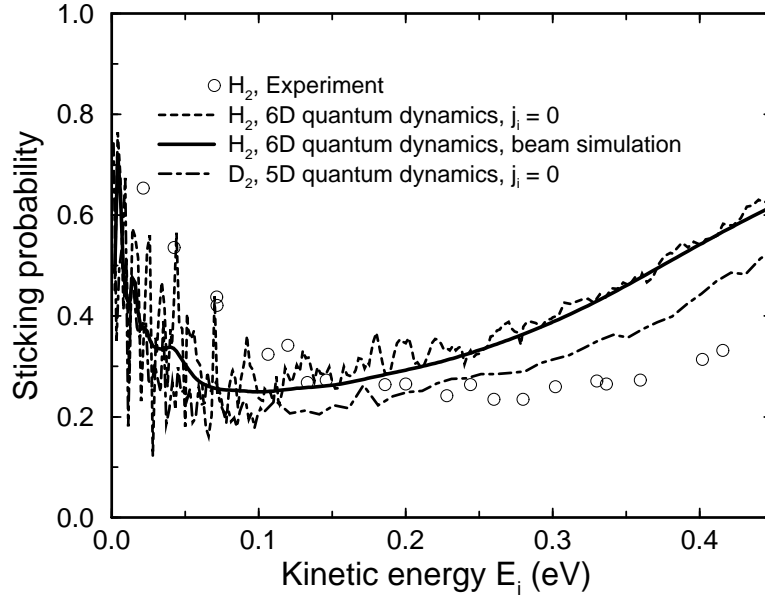


Fig. 2. Sticking probability versus kinetic energy for a hydrogen beam under normal incidence on a Pd(100) surface. Experiment (H_2): circles (from ref. [11]); theory: six-dimensional results for H_2 molecules initially in the rotational and vibrational ground state (dashed line) and with an initial rotational and energy distribution adequate for molecular beam experiments (solid line), and vibrationally adiabatic five-dimensional results for D_2 molecules initially in the rotational ground state (dash-dotted line).

resonances [26, 27]. These structures are known for a long time in He and H_2 scattering [28] and also in LEED [29]. For $\text{H}_2/\text{Pd}(100)$, however, measuring these oscillations is a very demanding task. They are very sensitive to surface imperfections like adatoms or steps [30] and therefore hard to detect [31]. Since we do not focus on these oscillations here, for the solid line in Fig. 2 we have assumed a velocity spread of the incoming beam typical for the experiment [11] so that the oscillations are smoothed out.

The initial decrease of the sticking probability found in the experiment is well-produced in the quantum dynamical calculations. The high sticking probability at low kinetic energies is caused by a steering effect: Slow molecules can very efficiently be steered to non-activated pathways towards dissociative adsorption by the attractive forces of the potential. This mechanism becomes less effective at higher kinetic energies where the molecules are too fast to be focused into favourable configurations towards dissociative adsorption. This causes the initial decrease of the sticking probability. If the kinetic energy is further increased, the

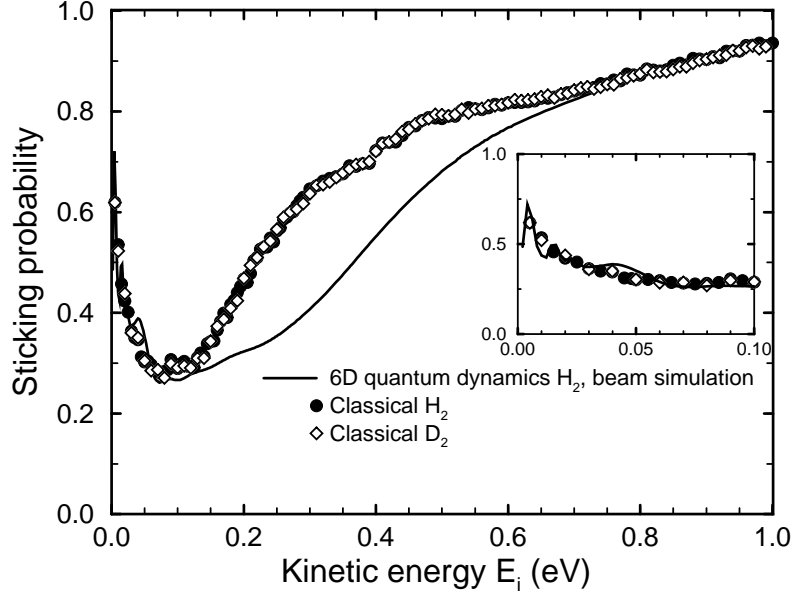


Fig. 3. Probability for dissociative adsorption versus kinetic translational energy for a H_2 beam under normal incidence on a clean $\text{Pd}(100)$ surface for non-rotating molecules. The solid line corresponds to the six-dimensional quantum dynamical results assuming an energy spread typical for beam experiments. The molecular dynamics results (H_2 : circles, D_2 : diamonds) have been obtained purely classical, i.e. without including zero-point energies in the initial conditions. The inset shows an enlargement of the results at low energies.

molecules will eventually have enough energy to directly traverse the barrier region leading to the final rise in the sticking probability.

In Fig. 3 we compare the averaged quantum mechanical sticking probability for H_2 with the results of classical trajectory calculations for H_2 and D_2 . The inset shows an enlargement of the results at low energies. The molecular dynamics calculations have been performed *without* any zero-point energies in the initial conditions. This allows us to truly differentiate between classical and quantum effects in the dynamics. First of all, the classical results do not show any oscillatory structure revealing that the oscillations are purely due to quantum mechanics. Furthermore, at low energies the classical results fall almost exactly upon the averaged quantum results. This shows that steering is a general concept and not restricted to quantum or classical dynamics. We attribute the difference between the classical and quantum results at the medium energy range to the influence of zero-point effects in the multi-dimensional interaction potential [32].

At very high energies, where zero-point effects play no role, quantum and classical results again agree.

Since the averaged quantum and the classical sticking probability agree in the low-energy regime, we can use classical trajectories to describe the steering mechanism. This is done in Fig. 4, where snapshots of two typical trajectories are shown. The initial conditions are chosen in such a way that the trajectories are restricted to the xz -plane.

The left trajectory illustrates the steering effect [10, 18]. The initial kinetic energy is $E_i = 0.01$ eV. Initially the molecular axis is almost perpendicular to the surface. In such a configuration the molecule cannot dissociate at the surface. But the molecule is so slow that the attractive forces can reorient the molecule so that it can follow a non-activated path towards dissociative adsorption.

In the case of the right trajectory, the initial conditions are the same as in the left one, except that the molecule has a higher kinetic energy of 0.12 eV. Due to the anisotropy of the PES the molecule also starts to rotate to a configuration parallel to the surface. However, now the molecule is so fast that it hits the repulsive wall of the potential before it is in a favorable configuration to dissociative adsorption. It is then scattered back into the gas-phase rotationally excited.

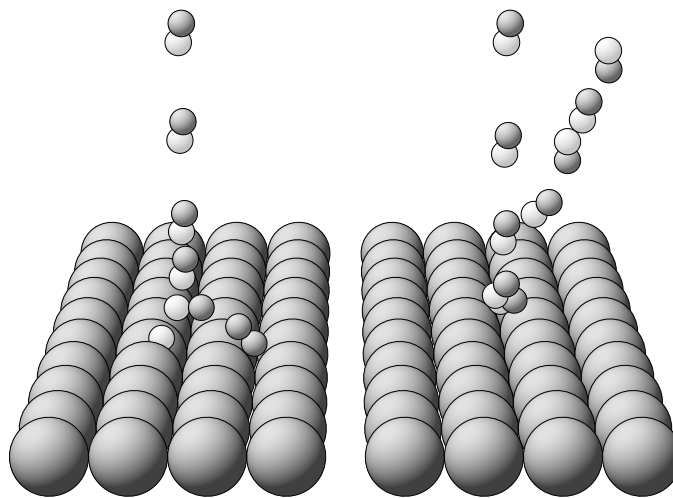


Fig. 4. Snapshots of classical trajectories of hydrogen molecules impinging on a Pd(100) surface. The initial conditions are chosen in such a way that the trajectories are restricted to the xz -plane. Left trajectory: initial kinetic energy $E_i = 0.01$ eV. Right trajectory: same initial conditions as in the left trajectory except that the molecule has a higher kinetic energy of 0.12 eV.

Finally we like to discuss the isotope effects in the dissociation of hydrogen on Pd(100). Fig. 3 shows that in classical dynamics there is practically no isotope effect between H_2 and D_2 in the sticking probability. As far as the low-energy regime is concerned, this seems surprising at a first glance, since D_2 is more inert than H_2 due to its higher mass. However, one has to keep in mind that at the same kinetic energy D_2 is slower than H_2 , so that there is more time for the steering forces to redirect the D_2 molecule. This compensating effect has also been found theoretically for the dissociation of hydrogen at W(100) [18].

In Fig. 2 we have also plotted the sticking probability of D_2 according to five-dimensional quantum dynamical calculations. Due to its higher mass the energy spacing between the quantum levels is smaller for D_2 than for H_2 . Therefore much more eigenfunctions in the expansion of the wavefunction have to be taken into account in the coupled-channel calculations for D_2 than for H_2 . This makes a six-dimensional quantum treatment of D_2 not feasible at the moment. However, we have already shown that the results of five-dimensional vibrationally adiabatic quantum calculations, where the molecules are not allowed to make vibrational transitions, are very close to the full six-dimensional results for the dissociation of hydrogen on Pd(100) [20]. Hence it is reasonable to compare five-dimensional results for D_2 with six-dimensional results for H_2 . The quantum dynamical sticking probabilities of D_2 are slightly smaller than those of H_2 . Since no such isotope effect is observed in the classical calculations (Fig. 3), this small difference has to be a quantum mechanical effect. We attribute it to the larger vibrational zero-point energy of H_2 which can effectively be used to traverse the barrier region [20, 32].

4 Conclusions

In conclusion, we reported a six-dimensional quantum and classical dynamical study of dissociative adsorption of $\text{H}_2/\text{Pd}(100)$. We have shown that the initial decrease of the sticking probability is due to a steering mechanism which is operative both in quantum and classical dynamics. The adsorption dynamics shows only a small isotope effect which is purely due to the quantum nature of hydrogen. Our results establish the importance of a high-dimensional dynamical treatment in order to understand reactions at surfaces.

References

- [1] K.D. Rendulic and A. Winkler, Surf. Sci. **299/300**, 261 (1994).
- [2] S. Holloway, Surf. Sci. **299/300**, 656 (1994).
- [3] G.R. Darling and S. Holloway, Rep. Prog. Phys. **58**, 1595 (1995).
- [4] A. Gross, Surf. Sci. **363**, 1 (1996).
- [5] B. Hammer, M. Scheffler, K.W. Jacobsen, and J.K. Nørskov, Phys. Rev. Lett. **73**, 1400 (1994).
- [6] J.A. White, D.M. Bird, M.C. Payne, and I. Stich, Phys. Rev. Lett. **73**, 1404 (1994).

- [7] S. Wilke and M. Scheffler, Surf. Sci. **329**, L605 (1995); Phys. Rev. B **53**, 4926 (1996).
- [8] S. Wilke and M. Scheffler, Phys. Rev. Lett. **76**, 3380 (1996)
- [9] G. Wiesenekker, G.J. Kroes, and E.J. Baerends, J. Chem. Phys. **104**, 7344 (1996).
- [10] A. Gross, S. Wilke, and M. Scheffler, Phys. Rev. Lett. **75**, 2718 (1995).
- [11] K. D. Rendulic, G. Anger, and A. Winkler, Surf. Sci. **208**, 404 (1989).
- [12] Ch. Resch, H. F. Berger, K. D. Rendulic, and E. Bertel, Surf. Sci. **316**, L1105 (1994).
- [13] H. F. Berger, Ch. Resch, E. Grösslinger, G. Eilmsteiner, A. Winkler, and K. D. Rendulic, Surf. Sci. **275**, L627 (1992).
- [14] D. A. Butler, B. E. Hayden, and J. D. Jones, Chem. Phys. Lett. **217**, 423 (1994).
- [15] P. Alnot, A. Cassuto, and D. A. King, Surf. Sci. **215**, 29 (1989).
- [16] D. A. Butler and B. E. Hayden, Chem. Phys. Lett. **232**, 542 (1995).
- [17] St. J. Dixon-Warren, A. T. Pasteur, and D. A. King, Surf. Rev. and Lett. **1**, 593 (1994).
- [18] M. Kay, G.R. Darling, S. Holloway, J.A. White, and D.M. Bird, Chem. Phys. Lett. **245**, 311 (1995).
- [19] A. Gross, S. Wilke, and M. Scheffler, Surf. Sci. **357/358**, 614 (1996).
- [20] A. Gross and M. Scheffler, Chem. Phys. Lett. **256**, 417 (1996).
- [21] J. P. Perdew, J. A. Chevary, S. H. Vosko, K. A. Jackson, M. R. Pederson, D. J. Singh, and C. Fiolhais, Phys. Rev. B **46**, 6671 (1992).
- [22] P. Blaha, K. Schwarz, and R. Augustyn, WIEN93, Technical University of Vienna 1993.
- [23] B. Kohler, S. Wilke, M. Scheffler, R. Kouba, and C. Ambrosch-Draxl, Comput. Phys. Commun. **94**, 31 (1996).
- [24] W. Brenig, T. Brunner, A. Gross, and R. Russ, Z. Phys. B **93**, 91 (1993).
- [25] W.H. Press, B.P. Flannery, S.A. Teukolsky, and W.T. Vetterling, *Numerical Recipes*, Cambridge University Press, Cambridge, 1989.
- [26] G.R. Darling and S. Holloway, J. Chem. Phys. **93**, 9145 (1990).
- [27] A. Gross, J. Chem. Phys. **102**, 5045 (1995).
- [28] R. Frisch and O. Stern, Z. Phys. **84**, 430 (1933).
- [29] J.B. Pendry, *Low energy electron diffraction*, Academic Press, London (1974), p. 112.
- [30] A. Gross and M. Scheffler, Phys. Rev. Lett. **77**, 405 (1996).
- [31] C.T. Rettner and D.J. Auerbach, Chem. Phys. Lett. **253**, 236 (1996).
- [32] A. Gross and M. Scheffler, to be published.